Environmental Science & Technology

pubs.acs.org/est

Article

# Multidirectional Fate Path Model to Connect Phosphorus Emissions with Freshwater Eutrophication Potential

Yujie Zhuang, Xin Liu, Jinhui Zhou, Hu Sheng, and Zengwei Yuan*

Cite This: *Environ. Sci. Technol.* 2024, 58, 11675−11684

Read Online

ACCESS | Metrics & More | Article Recommendations | Supporting Information

**ABSTRACT:** Excessive anthropogenic phosphorus (P) emissions put constant pressure on aquatic ecosystems. This pressure can be quantified as the freshwater eutrophication potential (FEP) by linking P emissions, P fate in environmental compartments, and the potentially disappeared fraction of species due to increase of P concentrations in freshwater. However, previous fate modeling on global and regional scales is mainly based on the eight-direction algorithm without distinguishing pollution sources. The algorithm fails to characterize the fate paths of point-source emissions via subsurface pipelines and wastewater treatment infrastructure, and exhibits suboptimal performance in accounting for multidirectional paths caused by river bifurcations, especially in flat terrains. Here we aim to improve the fate modeling by incorporating various fate paths and addressing multidirectional scenarios. We also update the P estimates by complementing potential untreated point-source emissions (PSu). The improved method is examined in a rapidly urbanizing area in Taihu Lake Basin, China in 2017 at a spatial resolution of 100 m × 100 m. Results show that the contribution of PSu on FEP (62.6%) is greater than that on P emissions (58.5%). The FEP is more spatially widely distributed with the improved fate modeling, facilitating targeted regulatory strategies tailored to local conditions.

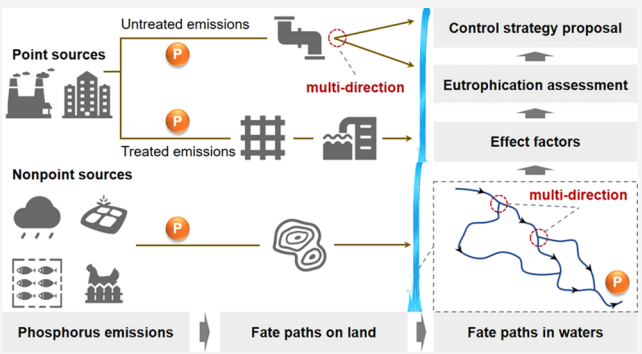


**KEYWORDS:** *nutrient, emission inventory, environmental fate, characterization factors, eutrophication assessment, environmental management*

## 1. INTRODUCTION

Phosphorus (P) is an essential element in nucleic acid synthesis and energy metabolism.[1] With rising populations and accelerating industrial activities, the annual extraction of phosphate ores is primarily aimed at supporting global food production through fertilizer manufacturing.[2,3] Yet, future projections predict an increasing disparity between food supply and demand.[4,5] Meanwhile, the excessive P input into aquatic systems surpasses the established planetary boundary,[6,7] leading to freshwater eutrophication[8] and biodiversity loss.[9] Experimental evidence shows that P limitation disrupts microbial processes governing nitrogen (N) transformation and carbon cycling,[10,11] highlighting the importance of curbing anthropogenic P emissions to alleviate freshwater eutrophication.[12] Given the constant pressure on aquatic ecosystems from P emissions, eutrophication assessment based on the potentially disappeared fraction (PDF) of heterotrophic species (including aquatic invertebrates and fish) could help to pinpoint the P hotspots and facilitate prioritizing regulatory interventions.[13,14]

An important basis for assessing the freshwater eutrophication potential (FEP) is the quantification of P emissions into recipient waters using nutrient models.[15] These models, such as Global NEWS,[16] MARINA,[17] and IMAGE-GNM,[18] have integrated empirical, statistical, and mechanistic components[15,19] to estimate P emissions due to human excretion and detergent usage on global[19,20] and regional[21,22] scales, leveraging their correlation with gross domestic product (GDP).[23] Untreated point-source emissions (PSu), previously assumed to be retained or lost,[19] have now been refined for inclusion in these models as detergents, human excreta, and farm manure.[22,24,25] Furthermore, substance flow analysis, an approach that focuses on resource development and utilization,[26,27] has been used to analyze the untreated emissions from P chemical industry.[28] However, in contrast to those conducted on large spatial scales, which are constrained by available data,[20,22] local studies often depend on on-site measurements.[29,30] Moreover, untreated emissions from various industries, excluding P chemicals, and untreated

Received: February 1, 2024
Revised: June 7, 2024
Accepted: June 10, 2024
Published: June 18, 2024





https://doi.org/10.1021/acs.est.4c01205
*Environ. Sci. Technol.* 2024, 58, 11675−11684

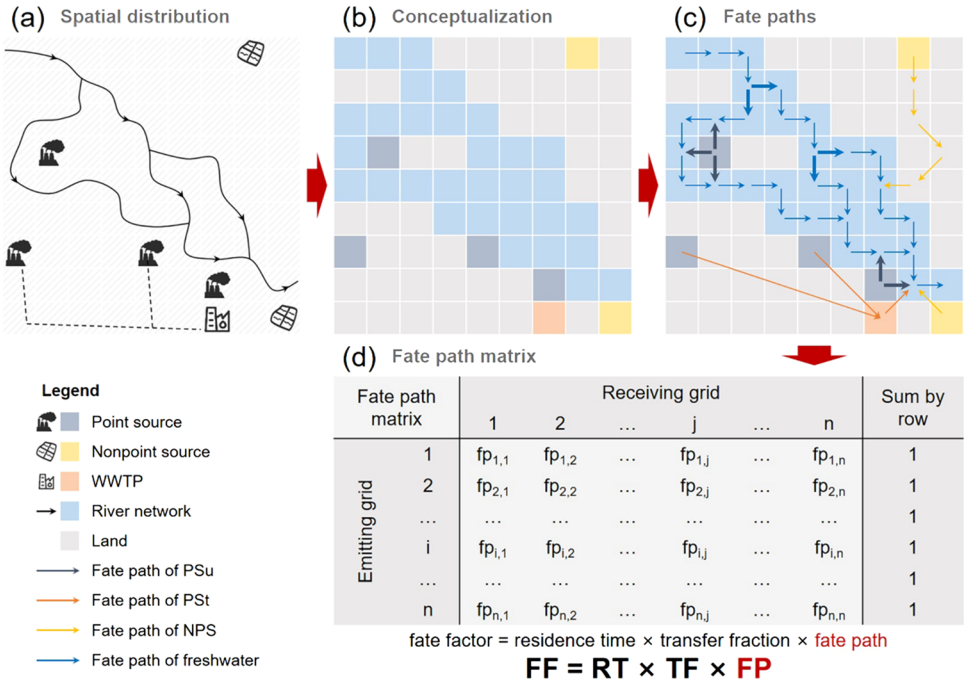


**Figure 1.** Improvement of fate factors. (a) Spatial distribution of pollution sources and water systems in reality. (b) Conceptualization of pollution sources and water systems as grids. (c) Diagram for fate paths of the untreated point-source emissions (PSu), the treated point-source emissions (PSt), the nonpoint-source emissions (NPS), and freshwater. Bold arrows indicate multiple directions. (d) Diagram of the fate path matrix.

components in sewage from other commercial consumption have not yet been addressed.

Fate modeling, which links human activities, P emissions, and P transport in environmental compartments,[31−33] is crucial for assessing the contribution of anthropogenic emissions to eutrophication.[34] Existing studies[28,35,36] typically use the eight-direction (D8) algorithm based on the Digital Elevation Model (DEM)[37] to trace the environmental fate paths of emissions from various sources. However, it is imperative to differentiate the fate paths of PSu, treated point-source emissions (PSt), and nonpoint-source emissions (NPS) as they are affected by different factors: pipelines, collection facilities, and topography, respectively. In addition, the fate paths of point-source emissions cannot be determined by the D8 algorithm due to subsurface pipelines and wastewater treatment infrastructure.[38] The D8 algorithm also performs worse in flat terrains with complex river networks and lacks the ability to characterize the bifurcation and connectivity of rivers, particularly at high spatial resolution.

To assess the FEP associated with human activities, we mainly make the following improvements to the existing methodology of P emissions estimation and environmental fate modeling:[28,35] (1) Estimating the untreated emissions from anthropogenic point sources using the Water Pollutant Loads Tracking (WPLT) model developed in our previous study.[39] (2) Spatially specifying how much of the P generated at each point source will eventually be emitted into freshwater based on a generation-weighted method. (3) Improving the simulation of P fate by distinguishing the fate paths of emissions from various sources and by considering the multidirectional paths caused by river bifurcations. The improved method is examined in a rapidly urbanizing area in Taihu Lake Basin, China in 2017 at a spatial resolution of 100 m × 100 m. It is of great significance for downscaling the assessment framework of large spatial scales to local scales. As FEP intensifies spatial differentiation of P emissions,[28] the improved method can provide practical guidance to facilitate more targeted regional regulatory strategies tailored to local conditions.

## 2. MATERIALS AND METHODS

Eutrophication is an important environmental impact category resulting from human activities.[40−42] FEP quantitatively reflects the fraction of species committed to extinction (i.e., the potentially disappeared fraction of species) in response to the constant pressure of P emissions on aquatic ecosystems.[28,43] It is a product of P emissions and characterization factors (CFs).[44,45] CFs theoretically consist of four factors in the cause-effect chain, namely, fate factors (FFs), exposure factors (XFs), effect factors (EFs), and damage factors (DFs).[46] Since XFs and DFs are optional,[15] here CFs are determined by both FFs and EFs following the general practice of existing studies.[28,35,44,47,48] FFs collectively reflect the persistence of nutrients in the environment, e.g., removal of P due to advection, retention, and water use.[49] EFs describe the relationship between the potentially disappeared fraction of species and the change in nutrient concentrations in waters.[14,50]

Based on the above computational framework, this study comprehensively considers the untreated P emissions from point sources, treated P emissions from point sources, and P emissions from nonpoint sources and distinguishes their fate paths. This not only enhances P emissions and FFs but also enables the eutrophication assessment to be traced from recipient waters to pollution sources, that is, quantifying the contribution of FEP from human activities. For ease of reading, the correspondence between the acronyms used in this study and their full terms is summarized in Table S1.

**2.1. Improvement of Phosphorus Emissions into Freshwater.** The WPLT model[39] is a process-based mass


https://doi.org/10.1021/acs.est.4c01205
Environ. Sci. Technol. 2024, 58, 11675−11684

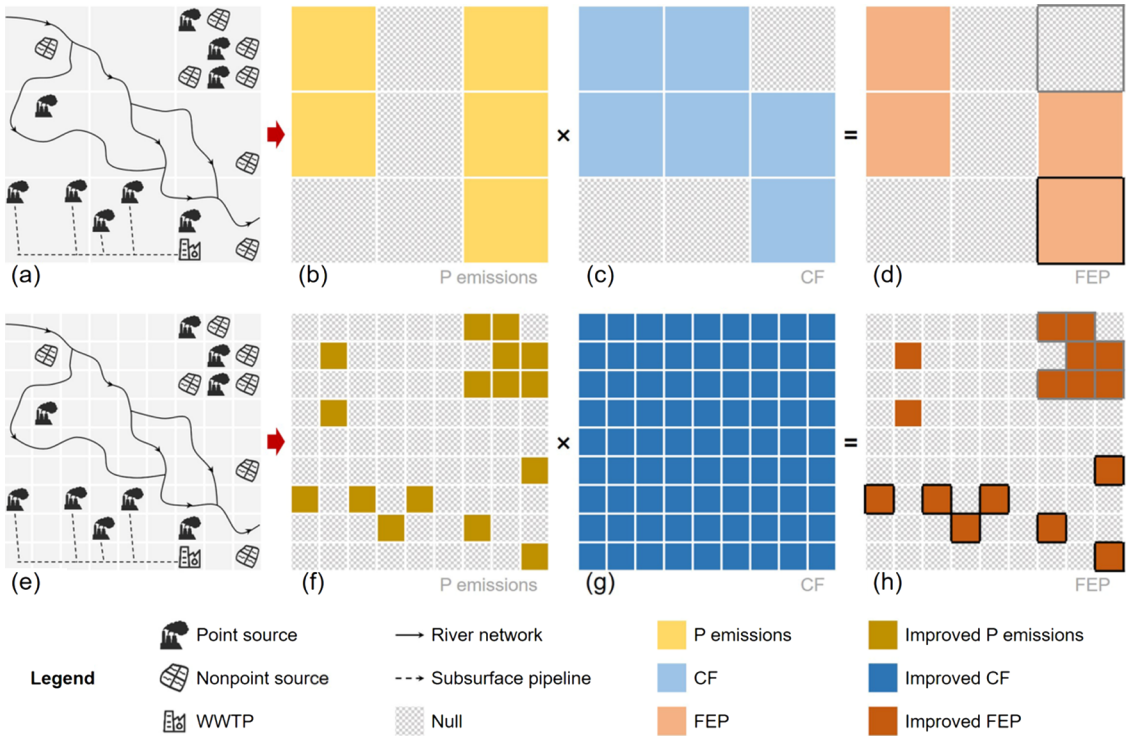


**Figure 2.** Improvement of the freshwater eutrophication potential (FEP). (a) Diagram of distribution within large-scale grids. (b) Phosphorus emissions (here in kg P) received by waters. (c) Characterization factors (CFs, here in PDF·day·m$^3$·kg P$^{1-}$) of water grids. (d) FEP (here in PDF·day·m$^3$) in recipient waters. (e) Diagram of distribution within small-scale grids. (f) P emissions from the initial sources as determined by the generation-weighted method. (g) CFs for all grids obtained from matrix operations of fate factors (FFs, here in day) and effect factors (EFs, here in PDF·m$^3$·kg P$^{1-}$). (h) The contribution of human activities to the FEP.

balance model that can trace the P pathway from sources to recipient waters through a life-cycle perspective, including major processes of generation, collection, treatment, and emission. It performs well in characterizing the pattern of P generation and independently analyzes the P generation and collection from point sources, thus identifying the substantial reductions between P generation and emission.

This study improves the simulation of P emissions into freshwater in two aspects: (1) Using the WPLT model to complement estimates of potential untreated P emissions from those anthropogenic point sources that have not yet been incorporated into existing nutrient models (Table S2). (2) Employing a generation-weighted method to spatially specify how much of the P generated at each point source will eventually be emitted into freshwater. The derivations are detailed in eqs S1 and S2, yielding the following results

$$PE_i^{PSu} = PG_i^{PS} \cdot (1 - F_u^{collection}) \cdot (1 - F^{subsurface\ pipeline}) \quad (1)$$

$$PE_i^{PSt} = PG_i^{PS} \cdot F_u^{collection} \cdot (1 - F^{subsurface\ pipeline}) \cdot (1 - F_u^{removal}) \quad (2)$$

where $PE_i^{PSu}$ and $PE_i^{PSt}$ (here both in kg P) are the untreated and treated P eventually emitted into freshwater from anthropogenic point sources in the grid $i$, respectively. $PG_i^{PS}$ (here in kg P) is the P generated from anthropogenic point sources in the grid $i$. $F_u^{collection}$ (dimensionless) is the P collection rate of the wastewater treatment plant (WWTP) $u$. $F^{subsurface\ pipeline}$ (dimensionless) is the P loss factor due to transport in subsurface pipelines. $F_u^{removal}$ (dimensionless) is the P removal efficiency of the WWTP $u$. All parameters used to calculate the P emissions are shown in Figure S1.

**2.2. Improvement of Fate Factors.** Considering the shortcomings of the D8 algorithm in simulating the fate paths of emissions,[28,35,36] this study develops a multidirectional fate path model to improve the FFs in three aspects (Figure 1): (1) Fate paths on land are modeled separately for each pollution source. (2) Fate paths in waters are improved by considering the complex morphology (i.e., the bifurcation and connectivity) of the river network, usually in flat terrains. (3) In order to facilitate expression and subsequent calculation, all P fate paths (dimensionless) from pollution sources to recipient waters are integrated into a matrix. In addition to the previously considered residence time (here in day) and the transfer fraction (dimensionless),[49] this matrix is considered as the third parameter to determine the FFs (here in day) in this study. The elements in the matrix represent the weights of fate paths, with each row summing up to 1.

Specifically, the fate path of PSu assumes that P enters waters from an artificial point source via subsurface pipelines following the nearest neighbor flow route. Note that this route may not be unique, that is, multiple directions may exist (bold gray arrows in Figure 1c). The fate path of PSt means that P enters the WWTP from an artificial point source via subsurface pipelines and is subsequently emitted into the nearest neighbor waters after treatment. The fate path of NPS is determined by the D8 algorithm. The fate path of freshwater can also be multidirectional due to river bifurcations (bold blue arrows in Figure 1c). The following steps are required to obtain the fate path matrix: (1) Pollution sources and water systems are conceptualized as grids in a projected coordinate system so that each grid has its own coordinates. (2) The distance between each point source emitting untreated P and all


https://doi.org/10.1021/acs.est.4c01205
Environ. Sci. Technol. 2024, 58, 11675−11684

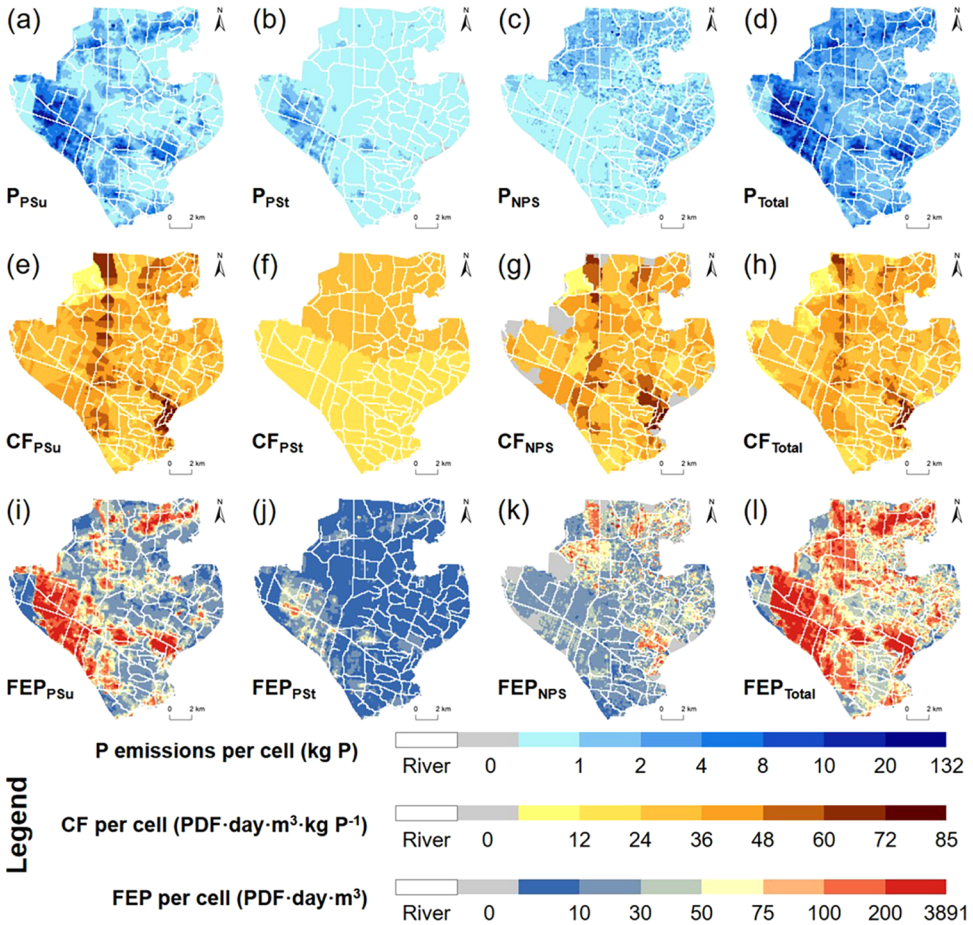


**Figure 3.** Spatial distribution of (a–d) P emissions, (e–h) characterization factors (CFs), and (i–l) freshwater eutrophication potential (FEP). PSu means the untreated point-source emissions. PSt means the treated point-source emissions. NPS means the nonpoint-source emissions. Total means the emissions from all pollution sources.

freshwater grids is calculated, and then the minimum distance is chosen as the fate path of P from each point source (emitting grid) to freshwater (receiving grid). (3) The pathway of P from each point source (emitting grid) to WWTP (receiving grid) is determined based on the coverage area of WWTPs. Similarly, the fate path of P from each WWTP (emitting grid) to freshwater (receiving grid) is determined by calculating the minimum distance. (4) The fate paths of P from nonpoint sources (emitting grid) to freshwater (receiving grid) are determined directly using the D8 algorithm based on DEM. (5) The fate path of P between freshwater grids is determined according to the morphology and directionality of the river network following main processes of vector extraction, value assignment, and bifurcation check (detailed in Section S1.2). The minimum distance is calculated as follows

$$f(i,j) = \underset{j=1}{\overset{n}{\text{minimum}}} \left[\sqrt{(x_i - x_j)^2 + (y_i - y_j)^2}\right] \quad (3)$$

where $f(i, j)$ represents the fate path from the emitting grid $i$ to the receiving grid $j$. The coordinates of the emitting grid $i$ and the receiving grid $j$ are $(x_i, y_i)$ and $(x_j, y_j)$, respectively. All parameters used to calculate the FFs are shown in Figure S2.

**2.3. Improvement of the Freshwater Eutrophication Potential.** Benefiting from the improvements in P emissions and FFs, as well as the high spatial resolution of the WPLT model, this study improves the eutrophication assessment (Figure 2) to quantify the contribution of various sources to the FEP (e.g., tracing the black-box grid in Figure 2d to the black-box grids in Figure 2h and the specific fate paths are shown in Figure 1c). The shift in perspective facilitates the application of computational frameworks at large scales (e.g., globe and nation) to small scales (e.g., city, county, and town), while providing a more comprehensive assessment at high spatial resolution. The improved method can address the contribution of terrestrial pollution sources to FEP (e.g., the gray-box grids in Figure 2h), which may be overlooked using the previous method[49] (e.g., the gray-box grid in Figure 2d). This is because, thanks to the improved fate paths, CFs now cover all grids. All parameters used to calculate the FEP are shown in Figure S4.

**2.4. Application of the Improved Method.** Taihu Lake, one of the five largest freshwater lakes located in the lower reaches of the Yangtze River in China, has been affected by eutrophication due to excessive anthropogenic P inputs from its surroundings.[51] In this study, after comprehensively considering the coverage area of WWTPs, administrative divisions, and river system distributions, a rapidly urbanizing area (120° 23′ 15″–120° 35′ 41″ E, 31° 27′ 23″–31° 38′ 30″ N) of 234 km$^2$ in Wuxi City in Taihu Lake Basin is selected as the study area (Figure S5). Further information on the study area is supplemented in Section S1.4. The improved method is applied to quantify the FEP contributed by human activities in


https://doi.org/10.1021/acs.est.4c01205
Environ. Sci. Technol. 2024, 58, 11675–11684

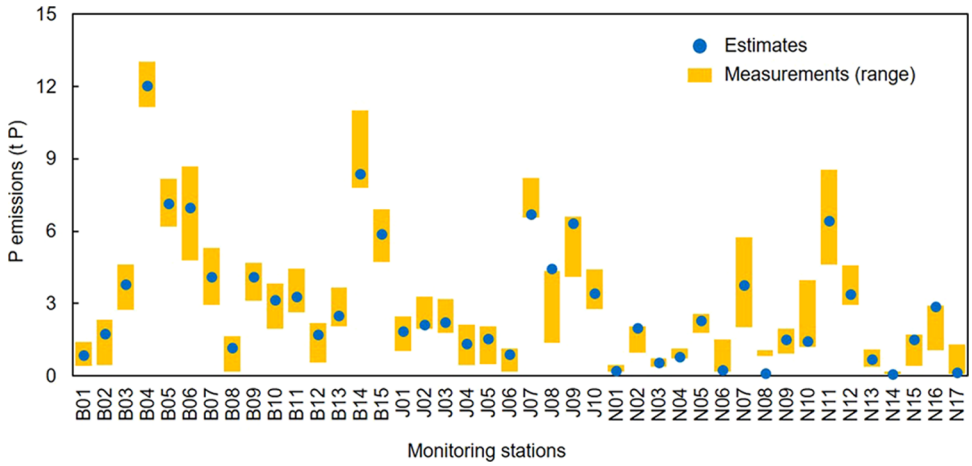


**Figure 4.** Comparison of P emissions into freshwater between model results and on-site measurements from monitoring stations.

this area in 2017 at a spatial resolution of 100 m × 100 m. The sources of the underlying parameters are detailed in Tables S3−S5.

## 3. RESULTS AND DISCUSSION

**3.1. Phosphorus Emissions into Freshwater.** In 2017, the P emitted into freshwater from all pollution sources in the study area was estimated at 69.2 tons. The spatial distribution of these emissions is illustrated in Figure 3, with PSu, PSt, and NPS contributing 58.5, 11.5, and 30.0%, respectively. To improve P emissions estimation, 4100 industrial enterprises in 34 categories are covered (Table S6). Furthermore, we sampled at the connections between residences and subsurface pipelines to include additional components other than human excreta and detergents in sewage. The samples comprehensively reflect pollution generation activities in residential areas, including human excretion, household cleaning, and commercial consumption (e.g., consumption in restaurants, car washes, and shopping malls).

Specifically, the hotspots of PSu and PSt both appear in built-up areas with high levels of urbanization, characterized by large population densities, industrial clusters, and developed commercial activities. However, there are some differences between the two. PSu is more prominent and has a wider coverage, which highlights the relatively high P removal efficiency of local WWTPs. According to our field interviews, the integrated P removal efficiency across the region was estimated to be 95.3%, maintaining a relatively high level in the range of 61.8−97.4% at the provincial level in China.[52] Meanwhile, the disparity in hotspots underscores that despite the regional integrated collection rate for wastewater achieving 89.2%, there is an urgent need for further enhancement of the collection system to prevent PSu, given it sets the pattern of spatial hotspots for the overall P emissions of the region.

Unlike hotspots of PSu and PSt, hotspots of NPS predominantly occur in suburban areas with lower levels of urbanization. These areas engage in intensive drainage activities from paddy farming, animal breeding, and aquaculture. The coverage of municipal pipe infrastructure in rural areas is relatively low, leading to the direct discharge of household sewage into waters. Furthermore, the residual chemical fertilizers and pesticides applied in these regions are easily flushed into waters through rainfall-induced runoff, thereby contributing to eutrophication.

**3.2. Characterization Factors.** In 2017, the spatial distribution of CFs associated with various sources in the study area is illustrated in Figure 3. The ranges of these CFs for PSu, PSt, NPS, and the total are 8.6−84.9, 20.9−28.9, 8.7−79.6, and 0.001−73.9 PDF·day·m$^3$·kg P$^{1-}$, respectively. The distribution of hotspots for the total CFs is dominated by that of PSu and NPS. It should be noted that, unlike the total P emissions, the total CFs are not obtained by adding the CFs of PSu, PSt, and NPS, but by dividing the total FEP by the total P emissions, reflecting the CFs of all sources in each grid.

The hotspots for the CFs of PSu are mainly located in the northern, central, and southeastern regions of the study area, implying that these regions are sensitive to anthropogenic P-related activities. In particular, the emission of P-containing wastewater into the water environment without treatment should be prohibited. To some extent, the CFs of PSt can reflect the rationality of WWTP outlet locations. The WWTPs in Meicun, Ehu, and Anzhen villages have a CF of 21.0, 20.9, and 28.9 PDF·day·m$^3$·kg P$^{1-}$, respectively. These CFs are all at relatively low levels, suggesting that the siting of these WWTP outlets is appropriate. However, from the perspective of protecting the water environment, it is also worth considering optimizing the outlet locations to further reduce the corresponding CFs without relocating the WWTPs.

The distribution of hotspots for the CFs of NPS (Figure 3g) is similar to that of PSu (Figure 3e), but the regions involved are smaller, indicating that the fate paths following the D8 algorithm overlap to some extent with those of nearest neighbors. It also suggests the need to optimize the paths of NPS into rivers to avoid sensitive areas, such as laying rainwater pipelines to reduce surface runoff, building canals to direct agricultural wastewater into rivers where CFs are relatively small, and locating aquaculture away from sensitive areas. The collection and treatment of P-containing wastewater from nonpoint sources in hotspot grids is also highly recommended. In addition to the hotspots, areas with a value of zero on land also deserve attention. While topography limits the wastewater of nonpoint sources from these areas to surface water through natural runoff, trapped wastewater may threaten groundwater quality through infiltration.[53]

CFs in land grids are affected by those in the nearby water grids under a certain flow path. The hotspots for CFs of the river system are located in the northern, central, and southeastern regions of the study area (Figure S6), where


https://doi.org/10.1021/acs.est.4c01205
Environ. Sci. Technol. 2024, 58, 11675−11684

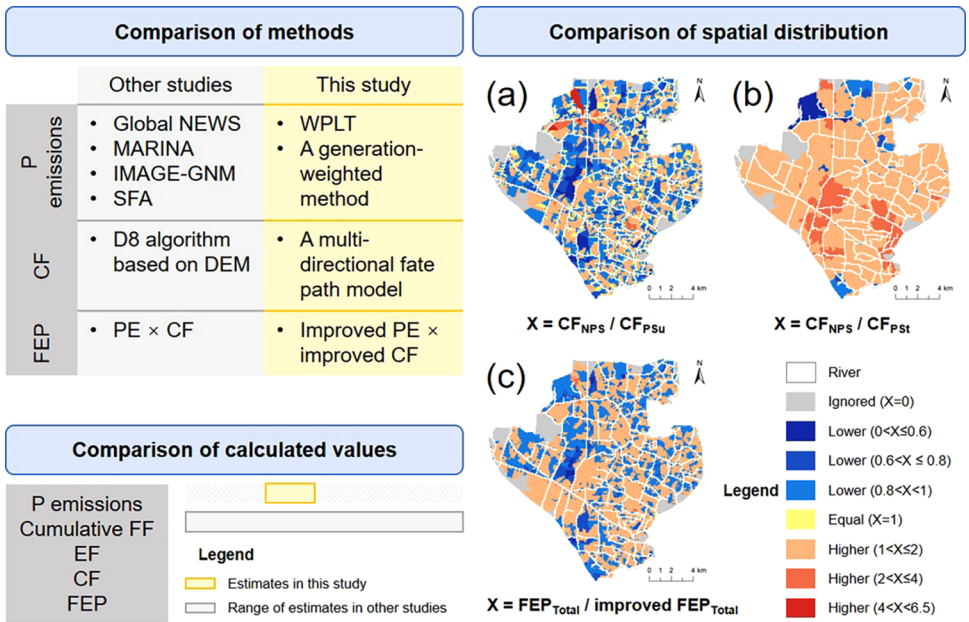


**Figure 5.** Comparisons of methods, calculated values, and spatial distribution. Spatial distribution of the changes in the characterization factor (CF) values without distinguishing the fate paths of (a) untreated and (b) treated emissions from point sources. (c) Spatial distribution of the changes in the freshwater eutrophication potential (FEP) values without distinguishing the fate paths of emissions from various sources.

the flow speeds of rivers do not exceed 0.06 $m \cdot s^{-1}$. At the same time, local waters with P concentrations ranging from approximately 0.13 to 0.91 $mg \cdot L^{-1}$ are not in an oligotrophic state. Rivers with relatively low P concentrations are more sensitive to additional P input, resulting in larger EFs. Therefore, additional attention needs to be paid to rivers with slow flow speeds and low P concentrations to prevent excessive anthropogenic P inputs that could lead to freshwater eutrophication.

**3.3. Freshwater Eutrophication Potential.** The total FEP of various sources in 2017 was about $2.3 \times 10^6$ PDF·day·$m^3$ for all grids, with PSu, PSt, and NPS contributing approximately 62.6, 7.8, and 29.6%, respectively. Their spatial patterns are shown in Figure 3.

The hotspot distribution for the FEP of point sources in the study area is primarily influenced by their P emissions, with CFs playing a minor role. However, the hotspot distribution for the FEP of NPS is affected by both P emissions and CFs. This suggests that regulatory strategies for point sources should prioritize controlling the P emissions, while those for nonpoint sources should address both the P emissions and CFs. The spatial hotspots of the total FEP are located in built-up areas with high levels of urbanization and along rivers characterized by slow flow speeds and low P concentrations.

**3.4. Comparison and Validation.** In our previous study, we have employed interactive crosschecks for the robustness of P inventory and conducted a quantitative analysis via Monte Carlo simulation, revealing an overall uncertainty range of −11.8 to 11.7%.[39] To further enhance the credibility of the multidirectional fate path model, a spatially explicit validation is carried out in this study. The model's performance, as assessed by comparing its outputs with data collected from various monitoring stations along the river network (Figure S5d), exhibits satisfactory agreement (Figure 4).

This study enhances the modeling of P fate path within the current computational framework (Figure 5), with the primary impact on spatial distribution rather than overall range of values (theoretically illustrated in Figure 2), thus facilitating the identification of spatial hotspots for local regulation. Given the geographical scope of the case area in this study only covers one to two grids as defined in the existing large-scale studies, it is challenging to conduct a direct spatial comparison. Therefore, we employ the default D8 algorithm, which is only used to calculate the CFs of NPS in the improved fate modeling, for all pollution sources. This allows us to derive an alternative spatial distribution of CFs and FEP so that the contribution of methodological improvements can be evaluated.

If the CFs of NPS are used to characterize point sources without distinguishing the fate paths of various sources, significant differences would be expected (Figure 5a,b). In this case, the grids where the CFs of PSu are significantly higher are located in the northeastern part of the study area, corresponding to values that are 4−6.5 times the original ones. Conversely, grids displaying values less than 0.6 times the original are mainly located in the northern, central, and southern parts. Meanwhile, the CFs of PSt increase in most grids, corresponding to values that are up to 3.8 times the original ones. The CFs of point sources in the western and southeastern parts of the study area cannot be directly characterized because the topography limits the pathway through natural runoff.

The total FEP is estimated to be $2.27 \times 10^6$ PDF·day·$m^3$ for all grids, closely aligning with the result of $2.28 \times 10^6$ PDF·day·$m^3$ obtained by distinguishing fate paths, as positive and negative deviations across the grids cancel out. However, the sum of the absolute values of deviations across all grids accounts for 15.9% of the total FEP calculated using the improved method. Figure 5c shows that failing to distinguish fate paths results in changes in the FEP values for nearly all grids, with the proportions of neglected, decreased, unchanged, and increased values at 7.7, 35.2, 0.1, and 57.0%, respectively. This indicates that the FEP induced by human activities is


https://doi.org/10.1021/acs.est.4c01205
Environ. Sci. Technol. 2024, 58, 11675−11684

more spatially widely distributed with the improved fate modeling.

Moreover, we evaluate the model's performance by comparing the numerical ranges of key essential intermediate variables (P emissions, cumulative FFs, EFs, and CFs) and final computational results (FEP) against those reported in previous studies (Tables S8 and S9). Specifically, the emission intensity for all sources (295 kg P·km$^{-2}$) is in acceptable discrepancies with estimates (102−350 kg P·km$^{-2}$) from other studies.[22,25,28,54] Several factors contribute to its occurrence, including regional economic disparities, differences in computational approaches, and the inclusion or exclusion of additional pollution source categories. For ease of general comparison, we aggregate the values of the cumulative FFs and CFs in this study to match the spatial resolution of other studies.[14,28,49,55,56] In this way, estimates of the cumulative FFs (6−54 days) are found to be within the range estimated by Helmes et al.[49] (0−more than 300 days), and within a small interval of that range. It remains in line with their finding that values are lower in coastal areas compared to upstream regions of large lakes or reservoirs.[49] This study area is located near the Yangtze River estuary, and the local water system does not involve lakes or reservoirs before entering Taihu Lake. Additionally, we have incorporated the sewage treatment modeling into the calculation of the removal rates caused by water use (eq S11) and considered the multidirectional fate of P in freshwater. The EFs (278−974 PDF·m$^3$·kg P$^{1-}$) estimated in this study are in good agreement with those estimated by Azevedo et al.[14] (0−1235 PDF·m$^3$·kg P$^{1-}$ for streams). Admissible differences can be attributed to the fact that Europe initiated long-term water environment management prior to China, resulting in lower P concentrations in local water bodies, which are more sensitive to additional P inputs, thus corresponding to larger EFs. We further compare the range of CFs estimated in this study with those from previous studies[14,28,56] and the aforementioned reasons may explain the tolerable difference between this study and others. Compared with the FEP estimated by Liu et al.[28] (0−$10^9$ PDF·year·m$^3$ at a spatial resolution of 5′ × 5′), our findings fall within a relatively lower range (0−3891 PDF·day·m$^3$ at a spatial resolution of 100 m × 100 m), resulting from the interplay between P emissions and CFs. The FEP in this study is primarily influenced by P emissions, whereas the FEP obtained by Liu et al.[28] is mainly driven by CFs. When considering lakes and reservoirs, significantly higher CFs are derived, as P remains longer in these water bodies, prolonging the exposure of nutrients to phytoplankton and facilitating autotrophic growth.[57] The disparities between our findings in FEP and those of Huang et al.[45] ($1.8 \times 10^{-8}$−$5.0 \times 10^{-5}$ PDF·year at a provincial level) and Scherer et al.[44] (0−more than $10^{-7}$ PDF·day·m$^3$·kg crop$^{-1}$ at a spatial resolution of 5′ × 5′) are mainly caused by the differing focus of study subjects. They specifically examined crop planting systems, whereas our research examines the broader scope of human activities. Overall, the results of this study are reliable and robust through the comparison of various perspectives.

**3.5. Spatial Statistical Analysis.** For all grids, both P emissions and FEP originating from human activities can undergo logarithmic transformation. This transformation allows for subsequent spatial statistical analysis through linear fitting. The efficacy of the fitting can be assessed through the characterization of the $R^2$ value.

The spatial statistical analysis of both P emissions and FEP from human activities for all grids is shown in Figure S8. After taking the logarithmic transformation, the P emissions and FEP exhibit relatively good fitting performance, with the overall $R^2$ above 0.78. The contribution of PSu on FEP (62.6%) is greater than that on P emissions (58.5%), indicating the importance of controlling PSu. The extreme value ratios (maximum divided by minimum) and the variances of FEP for various sources are significantly larger than those of P emissions (Table S10), demonstrating an increased spatial differentiation. Similar phenomena have been observed in other studies.[28,35,44]

**3.6. Scenario Analysis.** We apply a range of scenarios that were developed in our previous study[39] to assess the response to curbing P emissions under corresponding control measures. Specifically, (1) Scenario BAU (business as usual) does not take any control measures; (2) Scenario A1 upgrades the P removal efficiency of WWTPs to the highest practical level available for the year; (3) Scenario A2 involves collecting all untreated P-containing wastewater to the WWTPs and treating it at the existing removal level before emission; (4) Scenarios A3, A3−2, A3−3, and A3−4 reduce point-source generation by 10, 20, 30, and 40%, respectively; (5) Scenarios B1, B2, and B3 are combinations of A1+A2, A1+A3, and A2+A3, respectively; and (6) Scenario C is a synthesis of A1+A2+A3. Based on this, the improved method is applied in this study to further calculate the response to the reduction of FEP for each scenario (Figure S9). It is important to note that the results for the reduction efficiency of FEP are conservative in the sense that the emission reduction will also result in decreasing the P concentrations in waters, which will subsequently affect EFs, CFs, and ultimately FEP. Also, the effects of climate, social, and economic changes are not considered in the scenario setting.

The results show that P emissions and FEP are consistent in the order of reduction efficiency in each scenario. The combination of individual control measures has a synergistic effect rather than an antagonistic one. The series scenarios A3, A3−2, A3−3, and A3−4 show a positive correlation between the reduction in FEP and the reduction in both generation and emission. To further compare the resilience of each scenario, we calculate the ratio of FEP reduction efficiency to P emissions reduction efficiency for each of them. Scenario A2 has the highest value of 1.09, while scenario A1 ranks the bottom at 0.68 (Table S11). This is attributed to the significantly higher CFs of PSu compared to those of PSt, highlighting that enhancing the collection rate of P-containing wastewater takes precedence over improving the P removal efficiency of WWTPs.

**3.7. Environmental Implications and Limitations.** Accounting for potential untreated emissions from point sources has improved estimates of P emissions. The FFs are optimized by distinguishing the fate paths of emissions from various sources and by considering the multidirectional paths due to river bifurcations. Based on this, the FEP induced by human activities is more spatially widely distributed. Results from the study area reveal that the hotspots of P emissions are concentrated in areas with high levels of urbanization, characterized by large population densities, industrial clusters, and developed commercial activities. However, the local hotspots of FEP not only encompass these regions but also areas along slow-flowing rivers where P concentrations are low.



https://doi.org/10.1021/acs.est.4c01205
Environ. Sci. Technol. 2024, 58, 11675−11684

Scenario analysis of the study area indicates that enhancing the local collection rate of P-containing wastewater is most urgent, especially in areas with high CFs. It is also feasible, if economic and technical conditions permit, to continue to promote the upgrading of the treatment technology at WWTPs and the reduction of source generation, as these initiatives have synergistic effects when combined.

Additionally, some wastewater from nonpoint sources cannot enter surface water through natural runoff due to terrain limitations. Instead, the trapped wastewater may find its way into rivers and lakes via subsurface flows and other mechanisms after infiltration. The resulting eutrophication, although not addressed in this study, deserves further exploration in future studies. Finally, yet importantly, statistical analysis shows that the ratio of N to P in a given water body determines the limiting nutrient(s) for eutrophication.[58] Incorporating the stoichiometry of N and P[59] into the eutrophication assessment is a promising area for future refinement.

## ■ ASSOCIATED CONTENT

### Data Availability Statement

All data used in this study has been clarified in the manuscript.

### Supporting Information

The Supporting Information is available free of charge at https://pubs.acs.org/doi/10.1021/acs.est.4c01205.

Additional modeling details and results for phosphorus emissions, fate factors, and freshwater eutrophication potential, including comparison, validation, and analysis (PDF)

## ■ AUTHOR INFORMATION


### Corresponding Author

**Zengwei Yuan** − *State Key Laboratory of Pollution Control and Resource Reuse, School of the Environment, Nanjing University, Nanjing 210023, P. R. China;* orcid.org/0000-0002-6533-4170; Email: yuanzw@nju.edu.cn

### Authors

**Yujie Zhuang** − *State Key Laboratory of Pollution Control and Resource Reuse, School of the Environment, Nanjing University, Nanjing 210023, P. R. China*

**Xin Liu** − *State Key Laboratory of Pollution Control and Resource Reuse, School of the Environment, Nanjing University, Nanjing 210023, P. R. China*

**Jinhui Zhou** − *Institute of Environmental Sciences (CML), Leiden University, 2300 RA Leiden, The Netherlands;* orcid.org/0000-0001-8640-955X

**Hu Sheng** − *Key Laboratory of Watershed Geographic Sciences, Nanjing Institute of Geography and Limnology, Chinese Academy of Sciences, Nanjing 210008, P. R. China*

Complete contact information is available at: https://pubs.acs.org/10.1021/acs.est.4c01205


### Author Contributions

Conceptualization: Y.Z., Z.Y. Methodology: Y.Z. Software: Y.Z., H.S. Validation: Y.Z., X.L., H.S. Formal analysis: Y.Z., X.L., J.Z., H.S., Z.Y. Investigation: Y.Z., X.L. Resources: Z.Y. Data Curation: Y.Z., H.S. Writing—Original Draft: Y.Z. Writing—Review& Editing: Y.Z., X.L., J.Z., Z.Y. Visualization: Y.Z. Supervision: X.L., Z.Y. Project administration: Y.Z. Funding acquisition: Z.Y.

### Notes

The authors declare no competing financial interest.

## ■ ACKNOWLEDGMENTS

This study was financially supported by the National Science Fund for Distinguished Young Scholars (No. 41925004).

## ■ REFERENCES


(1) Walton, C. R.; Ewens, S.; Coates, J. D.; Blake, R. E.; Planavsky, N. J.; Reinhard, C.; Ju, P.; Hao, J.; Pasek, M. A. Phosphorus availability on the early Earth and the impacts of life. *Nat. Geosci.* **2023**, *16* (5), 399−409.

(2) Cordell, D.; Rosemarin, A.; Schröder, J. J.; Smit, A. L. Towards global phosphorus security: A systems framework for phosphorus recovery and reuse options. *Chemosphere* **2011**, *84* (6), 747−758.

(3) Demay, J.; Ringeval, B.; Pellerin, S.; Nesme, T. Half of global agricultural soil phosphorus fertility derived from anthropogenic sources. *Nat. Geosci.* **2023**, *16* (1), 69−74.

(4) Tian, X.; Engel, B. A.; Qian, H.; Hua, E.; Sun, S.; Wang, Y. Will reaching the maximum achievable yield potential meet future global food demand? *J. Cleaner Prod.* **2021**, *294*, No. 126285.

(5) Cheng, M.; Quan, J.; Yin, J.; Liu, X.; Yuan, Z.; Ma, L. High-resolution maps of intensive and extensive livestock production in China. *Resour. Environ. Sustain.* **2023**, *12*, No. 100104, DOI: 10.1016/j.resenv.2022.100104.

(6) Yuan, Z.; Jiang, S.; Sheng, H.; Liu, X.; Hua, H.; Liu, X.; Zhang, Y. Human perturbation of the global phosphorus cycle: Changes and consequences. *Environ. Sci. Technol.* **2018**, *52* (5), 2438−2450.

(7) Steffen, W.; Richardson, K.; Rockström, J.; Cornell, S. E.; Fetzer, I.; Bennett, E. M.; Biggs, R.; Carpenter, S. R.; de Vries, W.; de Wit, C. A.; Folke, C.; Gerten, D.; Heinke, J.; Mace, G. M.; Persson, L. M.; Ramanathan, V.; Reyers, B.; Sörlin, S. Planetary boundaries: Guiding human development on a changing planet. *Science* **2015**, *347* (6223), No. 1259855.

(8) Zhou, J.; Leavitt, P. R.; Zhang, Y.; Qin, B. Anthropogenic eutrophication of shallow lakes: Is it occasional? *Water Res.* **2022**, *221*, No. 118728.

(9) Vörösmarty, C. J.; McIntyre, P. B.; Gessner, M. O.; Dudgeon, D.; Prusevich, A.; Green, P.; Glidden, S.; Bunn, S. E.; Sullivan, C. A.; Liermann, C. R.; Davies, P. M. Global threats to human water security and river biodiversity. *Nature* **2010**, *467* (7315), 555−561.

(10) Sundareshwar, P. V.; Morris, J. T.; Koepfler, E. K.; Fornwalt, B. Phosphorus limitation of coastal ecosystem processes. *Science* **2003**, *299* (5606), 563−565.

(11) Thingstad, T. F.; Krom, M. D.; Mantoura, R. F. C.; Flaten, G. A. F.; Groom, S.; Herut, B.; Kress, N.; Law, C. S.; Pasternak, A.; Pitta, P.; Psarra, S.; Rassoulzadegan, F.; Tanaka, T.; Tselepides, A.; Wassmann, P.; Woodward, E. M. S.; Riser, C. W.; Zodiatis, G.; Zohary, T. Nature of phosphorus limitation in the ultraoligotrophic eastern Mediterranean. *Science* **2005**, *309* (5737), 1068−1071.

(12) Schindler, D. W.; Hecky, R. E.; Findlay, D. L.; Stainton, M. P.; Parker, B. R.; Paterson, M. J.; Beaty, K. G.; Lyng, M.; Kasian, S. E. M. Eutrophication of lakes cannot be controlled by reducing nitrogen input: Results of a 37-year whole-ecosystem experiment. *Proc. Natl. Acad. Sci. U.S.A.* **2008**, *105* (32), 11254−11258.

(13) Azevedo, L. B.; van Zelm, R.; Elshout, P. M. F.; Hendriks, A. J.; Leuven, R. S. E. W.; Struijs, J.; de Zwart, D.; Huijbregts, M. A. J. Species richness−phosphorus relationships for lakes and streams worldwide. *Glob. Ecol. Biogeogr.* **2013**, *22* (12), 1304−1314.

(14) Azevedo, L. B.; Henderson, A. D.; van Zelm, R.; Jolliet, O.; Huijbregts, M. A. J. Assessing the importance of spatial variability versus model choices in life cycle impact assessment: The case of freshwater eutrophication in Europe. *Environ. Sci. Technol.* **2013**, *47* (23), 13565−13570.

(15) Morelli, B.; Hawkins, T. R.; Niblick, B.; Henderson, A. D.; Golden, H. E.; Compton, J. E.; Cooter, E. J.; Bare, J. C. Critical review of eutrophication models for life cycle assessment. *Environ. Sci. Technol.* **2018**, *52* (17), 9562−9578.

(16) Seitzinger, S. P.; Harrison, J. A.; Dumont, E.; Beusen, A. H. W.; Bouwman, A. F.Sources and delivery of carbon, nitrogen, and phosphorus to the coastal zone: An overview of Global Nutrient Export from Watersheds (NEWS) models and their application *Glob. Biogeochem. Cycle* 2005 *19* (4), GB4S01. DOI: 10.1029/2005GB002606.
(17) Strokal, M.; Kroeze, C.; Wang, M.; Bai, Z.; Ma, L. The MARINA model (Model to Assess River Inputs of Nutrients to seAs): Model description and results for China. *Sci. Total Environ.* **2016**, *562*, 869−888.
(18) Beusen, A. H. W.; Van Beek, L. P. H.; Bouwman, A. F.; Mogollón, J. M.; Middelburg, J. J. Coupling global models for hydrology and nutrient loading to simulate nitrogen and phosphorus retention in surface water - description of IMAGE−GNM and analysis of performance. *Geosci. Model Dev.* **2015**, *8* (12), 4045−4067.
(19) Mayorga, E.; Seitzinger, S. P.; Harrison, J. A.; Dumont, E.; Beusen, A. H. W.; Bouwman, A. F.; Fekete, B. M.; Kroeze, C.; Van Drecht, G. Global Nutrient Export from WaterSheds 2 (NEWS 2): Model development and implementation. *Environ. Model. Softw.* **2010**, *25* (7), 837−853.
(20) Beusen, A. H. W.; Doelman, J. C.; Van Beek, L. P. H.; Van Puijenbroek, P. J. T. M.; Mogollón, J. M.; Van Grinsven, H. J. M.; Stehfest, E.; Van Vuuren, D. P.; Bouwman, A. F. Exploring river nitrogen and phosphorus loading and export to global coastal waters in the Shared Socio-economic pathways. *Glob. Environ. Change* **2022**, *72*, No. 102426.
(21) Strokal, M.; Ma, L.; Bai, Z.; Luan, S.; Kroeze, C.; Oenema, O.; Velthof, G.; Zhang, F. Alarming nutrient pollution of Chinese rivers as a result of agricultural transitions. *Environ. Res. Lett.* **2016**, *11* (2), 24014.
(22) Liu, X.; Beusen, A. H. W.; van Puijenbroek, P. J. T. M.; Zhang, X.; Wang, J.; van Hoek, W. J.; Bouwman, A. F. Exploring wastewater nitrogen and phosphorus flows in urban and rural areas in China for the period 1970 to 2015. *Sci. Total Environ.* **2024**, *907*, No. 168091.
(23) Van Drecht, G.; Bouwman, A. F.; Harrison, J.; Knoop, J. M.Global nitrogen and phosphate in urban wastewater for the period 1970 to 2050 *Glob. Biogeochem. Cycle* 2009 *23* (4), GB0A03. DOI: 10.1029/2009GB003458.
(24) van Puijenbroek, P. J. T. M.; Beusen, A. H. W.; Bouwman, A. F. Global nitrogen and phosphorus in urban waste water based on the Shared Socio-economic pathways. *J. Environ. Manage.* **2019**, *231*, 446−456.
(25) Chen, X.; Strokal, M.; Van Vliet, M. T. H.; Stuiver, J.; Wang, M.; Bai, Z.; Ma, L.; Kroeze, C. Multi-scale modeling of nutrient pollution in the rivers of China. *Environ. Sci. Technol.* **2019**, *53* (16), 9614−9625.
(26) Wu, H.; Zhang, Y.; Yuan, Z.; Gao, L. Phosphorus flow management of cropping system in Huainan, China, 1990−2012. *J. Cleaner Prod.* **2016**, *112*, 39−48.
(27) Jiang, S.; Yuan, Z. Phosphorus flow patterns in the Chaohu Watershed from 1978 to 2012. *Environ. Sci. Technol.* **2015**, *49* (24), 13973−13982.
(28) Liu, X.; Sheng, H.; Jiang, S.; Yuan, Z.; Zhang, C.; Elser, J. J. Intensification of phosphorus cycling in China since the 1600s. *Proc. Natl. Acad. Sci. U.S.A.* **2016**, *113* (10), 2609−2614.
(29) Yuan, Z.; Pang, Y.; Gao, J.; Liu, X.; Sheng, H.; Zhuang, Y. Improving quantification of rainfall runoff pollutant loads with consideration of path curb and field ridge. *Resour. Environ. Sustain.* **2021**, *6*, No. 100042.
(30) Ji, J.; Gao, J.; Xing, L.; Liu, X. High-resolution mapping of the rainfall runoff pollution: Case study of Shiwuli River watershed, China. *Environ. Sci. Pollut. Res.* **2023**, *30* (11), 28935−28946.
(31) de Andrade, M. C.; Ugaya, C. M. L.; de Almeida Neto, J. A.; Rodrigues, L. B. Regionalized phosphorus fate factors for freshwater eutrophication in Bahia, Brazil: An analysis of spatial and temporal variability. *Int. J. Life Cycle Assess.* **2021**, *26* (5), 879−898.
(32) Payen, S.; Ledgard, S. F. Aquatic eutrophication indicators in LCA: Methodological challenges illustrated using a case study in New Zealand. *J. Cleaner Prod.* **2017**, *168*, 1463−1472.
(33) Henderson, A. D.; Niblick, B.; Golden, H. E.; Bare, J. C. Modeling spatially resolved characterization factors for eutrophication potential in life cycle assessment. *Int. J. Life Cycle Assess.* **2021**, *26* (9), 1832−1846.
(34) Payen, S.; Falconer, S.; Carlson, B.; Yang, W.; Ledgard, S. Eutrophication and climate change impacts of a case study of New Zealand beef to the European market. *Sci. Total Environ.* **2020**, *710*, No. 136120.
(35) Tong, Y.; Zhang, W.; Wang, X.; Couture, R.; Larssen, T.; Zhao, Y.; Li, J.; Liang, H.; Liu, X.; Bu, X.; He, W.; Zhang, Q.; Lin, Y. Decline in Chinese lake phosphorus concentration accompanied by shift in sources since 2006. *Nat. Geosci.* **2017**, *10* (7), 507−511.
(36) Zhou, J.; Scherer, L.; van Bodegom, P. M.; Beusen, A.; Mogollón, J. M. Regionalized nitrogen fate in freshwater systems on a global scale. *J. Ind. Ecol.* **2022**, *26* (3), 907−922.
(37) Li, Z.; Yang, T.; Xu, C.; Shi, P.; Yong, B.; Huang, C.; Wang, C. Evaluating the area and position accuracy of surface water paths obtained by flow direction algorithms. *J. Hydrol.* **2020**, *583*, No. 124619.
(38) Jones, E. R.; Bierkens, M. F. P.; Wanders, N.; Sutanudjaja, E. H.; van Beek, L. P. H.; van Vliet, M. T. H. Current wastewater treatment targets are insufficient to protect surface water quality. *Commun. Earth Environ.* **2022**, *3* (1), 221 DOI: 10.1038/s43247-022-00554-y.
(39) Zhuang, Y.; Liu, X.; Yuan, Z.; Sheng, H.; Gao, J. A process-based model to track water pollutant generation at high resolution and its pathway to discharge. *Water Resour. Res.* **2023**, *59* (12), No. e2023WR034738.
(40) Verones, F.; Hellweg, S.; Antón, A.; Azevedo, L. B.; Chaudhary, A.; Cosme, N.; Cucurachi, S.; de Baan, L.; Dong, Y.; Fantke, P.; Golsteijn, L.; Hauschild, M.; Heijungs, R.; Jolliet, O.; Juraske, R.; Larsen, H.; Laurent, A.; Mutel, C. L.; Margni, M.; Núñez, M.; Owsianiak, M.; Pfister, S.; Ponsioen, T.; Preiss, P.; Rosenbaum, R. K.; Roy, P.; Sala, S.; Steinmann, Z.; van Zelm, R.; Van Dingenen, R.; Vieira, M.; Huijbregts, M. A. J. LC-IMPACT: A regionalized life cycle damage assessment method. *J. Ind. Ecol.* **2020**, *24* (6), 1201−1219.
(41) Balasuriya, B. T. G.; Ghose, A.; Gheewala, S. H.; Prapaspongsa, T. Assessment of eutrophication potential from fertiliser application in agricultural systems in Thailand. *Sci. Total Environ.* **2022**, *833*, No. 154993.
(42) O Brien, D.; Markiewicz-Keszycka, M.; Herron, J. Environmental impact of grass-based cattle farms: A life cycle assessment of nature-based diversification scenarios. *Resour. Environ. Sustain.* **2023**, *14*, No. 100126.
(43) Jin, Y.; Behrens, P.; Tukker, A.; Scherer, L. Biodiversity loss from freshwater use for China's electricity generation. *Environ. Sci. Technol.* **2022**, *56* (5), 3277−3287.
(44) Scherer, L.; Pfister, S. Modelling spatially explicit impacts from phosphorus emissions in agriculture. *Int. J. Life Cycle Assess.* **2015**, *20* (6), 785−795.
(45) Huang, J.; Xu, C.; Ridoutt, B. G.; Wang, X.; Ren, P. Nitrogen and phosphorus losses and eutrophication potential associated with fertilizer application to cropland in China. *J. Cleaner Prod.* **2017**, *159*, 171−179.
(46) Rosenbaum, R. K.; Margni, M.; Jolliet, O. A flexible matrix algebra framework for the multimedia multipathway modeling of emission to impacts. *Environ. Int.* **2007**, *33* (5), 624−634.
(47) Dong, Y.; Cheng, X.; Li, C.; Xu, L. Spatially eutrophication potential and policy implication of nitrogen emission for surface water: A case study in Guangzhou city, China. *J. Environ. Manage.* **2023**, *342*, No. 118336.
(48) Hellweg, S.; Milà i Canals, L. Emerging approaches, challenges and opportunities in life cycle assessment. *Science* **2014**, *344* (6188), 1109−1113.
(49) Helmes, R. J. K.; Huijbregts, M. A. J.; Henderson, A. D.; Jolliet, O. Spatially explicit fate factors of phosphorous emissions to freshwater at the global scale. *Int. J. Life Cycle Assess.* **2012**, *17* (5), 646−654.

(50) Zhou, J.; Mogollón, J. M.; van Bodegom, P. M.; Barbarossa, V.; Beusen, A. H. W.; Scherer, L. Effects of nitrogen emissions on fish species richness across the world's freshwater ecoregions. *Environ. Sci. Technol.* **2023**, *57* (22), 8347−8354.
(51) Huishu, L.; Qiuliang, L.; Xinyu, Z.; Haw, Y.; Hongyuan, W.; Limei, Z.; Hongbin, L.; Huang, J.; Tianzhi, R.; Jiaogen, Z.; Weiwen, Q. Effects of anthropogenic activities on long-term changes of nitrogen budget in a plain river network region: A case study in the Taihu Basin. *Sci. Total Environ.* **2018**, *645*, 1212−1220.
(52) Tong, Y.; Wang, M.; Peñuelas, J.; Liu, X.; Paerl, H. W.; Elser, J. J.; Sardans, J.; Couture, R.; Larssen, T.; Hu, H.; Dong, X.; He, W.; Zhang, W.; Wang, X.; Zhang, Y.; Liu, Y.; Zeng, S.; Kong, X.; Janssen, A. B. G.; Lin, Y. Improvement in municipal wastewater treatment alters lake nitrogen to phosphorus ratios in populated regions. *Proc. Natl. Acad. Sci. U.S.A.* **2020**, *117* (21), 11566−11572.
(53) Gurdak, J. J.; Qi, S. L. Vulnerability of recently recharged groundwater in principle aquifers of the United States to nitrate contamination. *Environ. Sci. Technol.* **2012**, *46* (11), 6004−6012.
(54) Zhang, L.; Wang, S.; Han, M.; He, Q.; Pan, G.; Wang, C. Nitrogen and phosphorus pollution in the western district of Wangyu River and counter-measures, Taihu Basin. *J. Lake Sci.* **2010**, *22* (3), 315−320 (in Chinese).
(55) Payen, S.; Cosme, N.; Elliott, A. H. Freshwater eutrophication: Spatially explicit fate factors for nitrogen and phosphorus emissions at the global scale. *Int. J. Life Cycle Assess.* **2021**, *26* (2), 388−401.
(56) Zhou, J.; Mogollón, J. M.; van Bodegom, P. M.; Beusen, A. H. W.; Scherer, L. Global regionalized characterization factors for phosphorus and nitrogen impacts on freshwater fish biodiversity. *Sci. Total Environ.* **2024**, *912*, No. 169108.
(57) Vannote, R. L.; Minshall, G. W.; Cummins, K. W.; Sedell, J. R.; Cushing, C. E. The river continuum concept. *Can. J. Fish. Aquat. Sci.* **1980**, *37* (1), 130−137.
(58) Qin, B.; Zhou, J.; Elser, J. J.; Gardner, W. S.; Deng, J.; Brookes, J. D. Water depth underpins the relative roles and fates of nitrogen and phosphorus in lakes. *Environ. Sci. Technol.* **2020**, *54* (6), 3191−3198.
(59) Elser, J. J.; Devlin, S. P.; Yu, J.; Baumann, A.; Church, M. J.; Dore, J. E.; Hall, R. O.; Hollar, M.; Johnson, T.; Vick-Majors, T.; White, C. Sustained stoichiometric imbalance and its ecological consequences in a large oligotrophic lake. *Proc. Natl. Acad. Sci. U.S.A.* **2022**, *119* (30), No. e2092699177.


https://doi.org/10.1021/acs.est.4c01205
*Environ. Sci. Technol.* 2024, 58, 11675−11684